Pramana – J. Phys. (2019) 93:83
https://doi.org/10.1007/s12043-019-1846-8

Ultrasonic wave propagation in thermoelectric ZrX_2 (X = S, Se) compounds

SHAKTI PRATAP SINGH[1], GAURAV SINGH[1], ALOK KUMAR VERMA[1,*], P K YADAWA[2] and R R YADAV[1]

[1]Physics Department, University of Allahabad, Allahabad 211 002, India
[2]Department of Physics, Prof. Rajendra Singh (Rajju Bhaiya) Institute of Physical Sciences for Study and Research, Veer Bahadur Singh Purvanchal University, Jaunpur 222 003, India
*Corresponding author. E-mail: alok9369@gmail.com

MS received 1 March 2019; revised 22 May 2019; accepted 18 June 2019

Abstract. In the present work, we have calculated temperature-dependent second- and third-order elastic constants (SOECs and TOECs) of thermoelectric zirconium disulphide (ZrS_2) and zirconium diselenide ($ZrSe_2$) using a simple interaction potential model. SOECs have been used for the calculation of ultrasonic velocity along different orientations of propagation. Thermal relaxation time and ultrasonic attenuation have been determined with the help of SOECs and thermal conductivity. Temperature-dependent specific heat, thermal energy density, elastic coupling constants and Grüneisen parameters are also calculated using SOECs and other parameters. The dominating cause behind ultrasonic attenuation, in the temperature range of 300–900 K, is the interaction of acoustical phonon and lattice phonon. In the present study, we observed that the thermal conductivity and energy density play significant roles in ultrasonic attenuation. Ultrasonic velocity and attenuation are correlated with other thermophysical properties extracting important information about the quality and nature of the materials which are useful for industrial applications.

Keywords. Elastic constant; ultrasonic attenuation; phonon–phonon interaction; thermal conductivity; Grüneisen parameter.

PACS Nos 43.35.cg; 62.20.Dc; 63.20.Kr

1. Introduction

Nowadays, most of the energy waste is in the form of heat. The thermoelectric (TE) technology may be an alternative and environment-friendly technology for energy conversion which directly converts this heat into electrical energy [1,2]. The efficiency of TE materials is defined as the dimensionless figure of merit (ZT) which is a symbol of TE performance. The figure of merit (ZT) is given by the formula $ZT = S^2\sigma T/k$, where S, σ, T and k stand for the Seebeck coefficient, electrical conductivity, temperature and thermal conductivity, respectively. The main challenging task for the research community is the lower efficiency of these devices because of low figure of merit (ZT). Conceptually, to obtain a better figure of merit, materials must have a high value of Seebeck coefficient with good electrical conduction property and low thermal conductivity [1–7].

Acoustics is a powerful tool to study the properties of different types of materials. Ultrasonics is a non-destructive and useful technique for determining the structural integrity of materials [8,9]. The ultrasonic technique can be used for detecting discontinuities, measuring thickness, studying metallurgy, detecting damage in composites and determining elastic properties along with other thermophysical properties of materials. Nonlinear elastic properties (second- and third-order elastic constants (SOEC and TOEC)) can be utilised to determine ultrasonic scientific parameters like attenuation and to provide information about the microstructural features of materials [10,11].

In the race for high-performance TE materials, semiconducting transition metal dichalcogenides (TMDCs) from group IVB have attracted great interest due to their small thermal conductivity. In our present evaluation, we have studied ZrS_2 and $ZrSe_2$ which have a hexagonal close-packed (HCP) structure with lattice

Published online: 05 September 2019

constants $a = b = 3.69$ Å and axial ratio $p = 1.62$ and $a = b = 3.80$ Å and axial ratio $p = 1.66$, respectively [2]. The thermal conductivity of ZrX_2 has been reported by Ōnuki *et al* [4] and the Raman spectra of ZrX_2 have been reported by Valero *et al* [7]. Many other investigations also have been made on its superconducting behaviour but, to the best of our knowledge, no theoretical and experimental studies have been done on the ultrasonic attenuation in ZrX_2. The lack of information on the ultrasonic properties of ZrX_2 is the source of inspiration for the present study.

2. Theory

This section is divided into three phases: the first phase illustrates the theoretical approach to SOECs and TOECs, the second phase discusses orientation-dependent ultrasonic velocities and the third phase describes the theoretical approach for the determination of ultrasonic attenuation due to the phonon–phonon interaction and thermoelastic relaxation mechanisms.

2.1 *Theoretical approach for the calculation of higher-order elastic constants*

A general definition of elastic coefficients of any order is the partial derivative hermodynamic potential of the medium subjected to finite deformation. The elastic constant of nth order [12] is defined as:

$$C_{ijklmn\ldots} = \frac{\partial^n U}{\partial\eta_{ij}\partial\eta_{kl}\partial\eta_{mn}\ldots}, \tag{1}$$

where U is the elastic energy density and η_{ij} is a component of strain tensor.

The potential energy per unit cell up to second nearest neighbour is written as follows:

$$U_2 + U_3 = \sum_{I=1}^{6} U(r_I) + \sum_{J=1}^{6} U(r_J), \tag{2}$$

where I refers to atoms in the basal plane and J refers to atoms above and below the basal plane. Under homogeneous deformation, the interatomic vectors in undeformed state (r) and deformed state (r') are related as: $[(r')^2 - (r)^2 = 2\Theta]$.

The energy density U can be explained in terms of Θ as [13–15]:

$$U_n = (2V_c)^{-1} \sum \frac{1}{n!}\Theta^n D^n \varphi(r). \tag{3}$$

Using eqs (2) and (3), the energy density U involving cubic terms can be written as:

$$\begin{aligned} U_2 + U_3 = (2V_c)^{-1} &\left[\sum_{I=1}^{6} \frac{1}{2!}\Theta_I^2 D^2\varphi(r_I) + \sum_{J=1}^{6} \frac{1}{2!}\Theta_J^2 D^2\varphi(r_J)\right] \\ &+(2V_c)^{-1}\left[\sum_{I=1}^{6} \frac{1}{3!}\Theta_I^3 D^3\varphi(r_I) + \sum_{J=1}^{6} \frac{1}{3!}\Theta_J^3 D^3\varphi(r_J)\right], \end{aligned} \tag{4}$$

where $V_c = [3^{1/2}/2]a^2c$ stands for the volume of the elementary cell and $D = R^{-1}\mathrm{d}/\mathrm{d}R$. $\varphi(r)$ is the interaction potential and is given by the following equation as [16–19]:

$$\varphi(r) = -\frac{a_0}{r^m} + \frac{b_0}{r^n}, \tag{5}$$

where a_0, b_0 are constants; m, n are integers and r is the distance between atoms. Comparison of crystal symmetry leads six second and ten third order elastic constants (SOECs and TOECs) respectively.

The second-order (C_{IJ}) and third-order (C_{IJK}) elastic constants of the hexagonal material can be written as follows [17,18]:

$$\left.\begin{array}{ll} C_{11} = 24.1p^4C', & C_{12} = 5.918p^4C' \\ C_{13} = 1.925p^6C', & C_{33} = 3.464p^8C' \\ C_{44} = 2.309p^4C', & C_{66} = 9.851p^4C' \\ C_{111} = 126.9p^2B + 8.853p^4C' & \\ C_{112} = 19.168p^2B - 1.61p^4C' & \\ C_{113} = 1.924p^4B + 1.155p^6C' & \\ C_{123} = 1.617p^4B - 1.155p^6C' & \\ C_{133} = 3.695p^6B, & C_{155} = 1.539p^4B \\ C_{144} = 2.309p^4B, & C_{344} = 3.464p^6B \\ C_{222} = 101.039p^2B + 9.007p^4C' & \\ C_{333} = 5.196p^6B & \end{array}\right\}, \tag{6}$$

where $p = c/a$ is called the axial ratio, $C' = \chi a/p^5$, $B = \psi a^3/p^3$, $\chi = 1/8[\{nb_0(n-m)\}/\{a^{n+4}\}]$, $\Psi = -\chi/\{6a^2(m+n+6)\}$ and c is the height of the unit cell. The harmonic and anharmonic parameters (χ and ψ) are calculated using one reasonable value of SOECs, the basal plane distance (a) and axial ratio (p).

2.2 *Ultrasonic velocities*

The anisotropic and mechanical properties of solids can be understood with the knowledge of ultrasonic velocity because the velocity is related to the higher-order elastic constants. On the basis of the mode of atomic vibration, ultrasonic velocities are divided into three types:

one longitudinal (long.) wave and two shear waves for each direction of propagation of waves in HCP crystals [18–20].

The ultrasonic velocities as a function of the angle between the direction of propagation and unique axis for HCP-structured materials are given as follows:

$$\left.\begin{aligned} V_1^2 &= \{C_{33}\cos^2\theta + C_{11}\sin^2\theta + C_{44} \\ &\quad + \{[C_{11}\sin^2\theta - C_{33}\cos^2\theta \\ &\quad + C_{44}(\cos^2\theta - \sin^2\theta)]^2 \\ &\quad + 4\cos^2\theta\sin^2\theta(C_{13}+C_{44})^2\}^{1/2}\}/2\rho \\ V_2^2 &= \{C_{33}\cos^2\theta + C_{11}\sin^2\theta + C_{44} \\ &\quad - \{[C_{11}\sin^2\theta - C_{33}\cos^2\theta + C_{44}(\cos^2\theta \\ &\quad - \sin^2\theta)]^2 + 4\cos^2\theta\sin^2\theta(C_{13} \\ &\quad + C_{44})^2\}^{1/2}\}/2\rho \\ V_3^2 &= \{C_{44}\cos^2\theta + C_{66}\sin^2\theta\}/\rho \end{aligned}\right\}, \quad (7)$$

where V_1, V_2 and V_3 are the longitudinal, quasishear and shear wave velocities, ρ and θ are the density of the material and angle with the unique axis (z-axis) of the crystal, respectively.

2.3 *Ultrasonic attenuation and allied parameters*

The two dominant processes that will give rise to appreciable ultrasonic attenuation at higher temperatures are the phonon–phonon interaction (Akhieser-type damping) and thermoelastic loss and given by the following equation [21–23]:

$$(\alpha/f^2)_{\mathrm{Akh}} = \frac{4\pi^2\tau E_0(D/3)}{2\rho V^3}, \quad (8)$$

where f is the frequency of the ultrasonic wave, V is the velocity of the ultrasonic wave and E_0 is the thermal energy density. The acoustic coupling constant D is the measure of the acoustic energy converted into thermal energy and is given as [22]

$$D = 3(3E_0\langle(\gamma_i^j)^2\rangle - \langle\gamma_i^j\rangle^2 C_V T)/E_0, \quad (9)$$

where C_{V} is the specific heat per unit volume of the material, T is the temperature, γ_i^j is the Grüneisen number, i and j are the mode and direction of propagation, respectively.

Mason [24] has used Grüneisen constants $\langle\gamma_i^j\rangle$, which are directly related to SOECs and TOECs. This approach is found to be very useful for estimating ultrasonic attenuation in various materials. Burgger has derived a formula for γ_i^j in the form of tensor notation as [25,26]

$$-\gamma_i^j = -\gamma_i^{jk} = U_j U_k + \frac{N_p N_q}{2C'}(C_{jkpq} + U_r U_s C_{jkprqs}), \quad (10)$$

where j and k are the two index symbols for the strain, U_j, U_k, etc. are the direction cosine of the polarisation direction, N_p, N_q are the direction cosine of the propagation direction and C' is the effective elastic modulus associated with the direction of propagation of the wave. C_{jkpq} and C_{jkprqs} are the SOECs and TOECs, respectively, in tensor notation.

Due to the propagation of ultrasonic wave through a material, the equilibrium of phonon distribution gets disturbed. It takes some time for the re-establishment of equilibrium of the thermal phonons. This time is known as the thermal relaxation time τ and is given by the following equation [23]:

$$\tau = \tau_{\mathrm{S}} = \tau_{\mathrm{L}}/2 = \frac{3k}{C_{\mathrm{V}}V_{\mathrm{D}}^2}, \quad (11)$$

where τ_{L} and τ_{S} are the thermal relaxation time for the longitudinal wave and shear wave, respectively, k is the thermal conductivity and V_{D} is the Debye average velocity. For the HCP-structured crystal, the Debye average velocity along any angle with the unique axis is given by the following equation [17,18]:

$$V_{\mathrm{D}} = \left[\frac{1}{3}\left(\frac{1}{V_1^3} + \frac{1}{V_2^3} + \frac{1}{V_3^3}\right)\right]^{-1/3}. \quad (12)$$

The thermoelastic loss $(\alpha)_{\mathrm{Th}}$ is calculated using the following equation:

$$(\alpha/f^2)_{\mathrm{Th}} = 4\pi^2\langle\gamma_i^j\rangle^2\frac{kT}{2\rho V_{\mathrm{L}}^5}. \quad (13)$$

The total attenuation is given as [17,18,21]

$$(\alpha/f^2)_{\mathrm{Total}} = (\alpha/f^2)_{\mathrm{Th}} + (\alpha/f^2)_{\mathrm{L}} + (\alpha/f^2)_{\mathrm{S}}, \quad (14)$$

where $(\alpha/f^2)_{\mathrm{Th}}$ is the thermoelastic loss and $(\alpha/f^2)_{\mathrm{L}}$ and $(\alpha/f^2)_{\mathrm{S}}$ are the ultrasonic attenuation coefficients for the longitudinal wave and shear wave, respectively.

3. Results and discussion

The SOECs and TOECs of ZrS_2 and $ZrSe_2$ are calculated and are presented in tables 1 and 2, respectively.

The elastic constants provide better information on the durability and the stiffness of the crystal. The SOECs (C_{11} and C_{33}) help with measuring the resistance towards linear compression in the a and c directions. In our evaluation the value of C_{11} is higher than that of C_{33} for ZrS_2 at all temperatures which means the c-axis will be more compressible than the a-axis. In the case of $ZrSe_2$ the value of C_{11} is less than C_{33}, which indicates that the a-axis will be more compressible than the c-axis. The other SOEC C_{44} can give information about the

Table 1. SOECs and TOECs (10^{10} N m^{-2}) vs. temperature T (K) of ZrS_2.

T(K)	300	400	500	600	700	800	900
C_{11}	130.7	127.1	123.6	120.2	116.9	113.8	110.7
C_{12}	64.1	62.4	60.7	59.0	57.4	55.9	54.4
C_{13}	54.8	53.4	52.0	50.6	49.3	48.0	46.8
C_{33}	129.4	126.4	123.2	120.2	117.2	114.3	111.5
C_{44}	32.8	32.0	31.1	30.3	29.6	28.8	28.0
C_{66}	51.2	49.8	48.4	47.1	45.8	44.6	43.4
C_{111}	− 2131.6	− 2072.1	− 2015.7	− 1961	− 1907.8	−1856.3	− 1806.3
C_{112}	− 346.7	− 337.0	− 327.8	− 318.9	− 310.7	− 301.9	− 293.7
C_{113}	− 140.5	− 136.9	− 133.4	− 129.9	− 126.5	− 123.3	− 120.1
C_{123}	− 89.3	− 87.0	− 84.7	− 82.5	− 80.4	− 78.3	− 76.3
C_{133}	− 437.1	− 427.0	− 416.4	− 406.1	− 396.9	− 386.3	− 376.8
C_{344}	− 409.7	− 400.3	− 390.4	− 380.7	− 371.3	− 362.1	− 353.2
C_{144}	− 104.1	− 101.4	− 98.7	− 96.2	− 93.7	− 91.3	− 88.9
C_{155}	− 69.7	− 67.6	− 65.8	− 64.1	− 62.4	− 60.8	− 59.2
C_{222}	− 1686.6	− 1639.5	− 1594.9	− 1551.6	− 1509.5	1468.7	− 1429.2
C_{333}	− 1613.2	− 1579.8	− 1542.5	− 1506.1	− 1470.8	− 1436.3	− 1402.8

Table 2. SOECs and TOECs (10^{10} N m^{-2}) vs. temperature T (K) of $ZrSe_2$.

T(K)	300	400	500	600	700	800	900
C_{11}	103.1	100.4	97.7	95.2	92.7	90.2	87.9
C_{12}	50.6	49.3	48.0	46.7	45.5	44.3	43.1
C_{13}	45.4	44.2	43.1	42.0	41.0	39.9	38.9
C_{33}	112.6	109.9	107.1	104.6	102.1	99.7	97.3
C_{44}	27.2	26.5	25.8	25.2	24.5	23.9	23.3
C_{66}	40.4	39.3	38.3	37.3	36.3	35.4	34.4
C_{111}	− 1682.7	− 1638.1	− 1594.7	− 1552.6	− 1511.8	− 1472.2	− 1499.5
C_{112}	− 273.6	− 266.4	− 259.3	− 252.5	− 245.8	− 299.4	− 233.1
C_{113}	− 116.5	− 113.5	− 110.6	− 107.9	− 105.1	− 102.5	− 99.9
C_{123}	− 74.0	− 72.1	− 70.3	− 68.5	− 66.8	− 65.1	− 63.5
C_{133}	− 380.4	− 371.2	− 362.2	− 353.5	− 345.0	− 336.8	− 328.8
C_{344}	− 356.6	− 348.0	− 339.6	− 313.4	− 323.5	− 315.7	− 308.2
C_{144}	− 86.2	− 84.8	− 81.9	− 79.8	− 77.8	− 75.9	− 74.0
C_{155}	− 57.5	− 56.0	− 54.6	− 53.2	− 51.9	− 50.6	− 49.3
C_{222}	− 1331.4	− 1296.1	− 1261.8	− 1228.5	− 1196.1	− 1164.7	− 1134.2
C_{333}	− 1474.1	− 1440.2	− 1407.2	− 1375.0	− 1343.7	− 1313.1	− 1283.3

hardness of the material. From tables 1 and 2, it is seen that the value of TOEC is negative. The negative values of the TOECs indicate the negative strain in the crystals.

The calculated values of the SOECs of ZrS_2 and $ZrSe_2$ at room temperature are compared with those obtained from the literature. The values of C_{11} and C_{44} for ZrS_2 are 130.7 and 32.8 GPa from the calculations of the present study while 131.4 and 52.9 GPa were the values obtained by Zhao *et al* [2]. Also the values of C_{11} and C_{44} for $ZrSe_2$ are 103.1 and 27.2 GPa from the calculations of the present study while 104.6 and 41.6 GPa were the values obtained by Zhao *et al* [2]. The comparison shows that some of the calculated values of higher-order elastic constants are in good agreement with previous predictions. However, the TOECs could not be compared because of the lack of reported data in the literature, but all the values of TOEC are negative that were reported in other HCP-structured materials like third-group nitrides, aluminium nitride, zinc sulphide and lead telluride [18,21–23]. Hence our theoretical approach for the calculation of nonlinear elastic constants for HCP-structured ZrS_2 and $ZrSe_2$ is justified and validated.

Some other thermophysical properties like energy density (E_0), specific heat per unit volume (C_V), ultrasonic velocities (longitudinal (V_L), shear (V_S) and Debye average velocity (V_D)) and thermal relaxation time (τ) have also been evaluated for ZrS_2 and $ZrSe_2$ and the evaluated values are presented in tables 3 and 4, respectively.

Table 3. Density ρ (10^3 kg m^{-3}), C_V (10^6 J m^{-3} K^{-1}), E_0 (10^9 J m^{-3}), thermal conductivity k (W m^{-1} K^{-1}), longitudinal velocity (10^3 m s^{-1}), shear velocity (10^3 m s^{-1}), Debye average velocity (10^3 m s^{-1}) and relaxation time (10^{-12} s) vs. temperature T(K) of ZrS_2.

T(K)	ρ	C_V	E_0	k	V_L	V_S	V_D	τ
300	3.824	5.861	1.245	18.00	5.817	2.931	3.245	8.842
400	3.823	6.005	1.838	13.00	5.750	2.894	3.204	6.517
500	3.822	6.044	2.439	11.00	5.679	2.856	3.163	5.554
600	3.821	6.074	3.045	8.50	5.609	2.820	3.122	4.305
700	3.820	6.103	3.666	7.50	5.540	2.783	3.082	3.879
800	3.819	6.122	4.270	6.00	5.477	2.748	3.044	3.225
900	3.818	6.121	4.877	5.30	5.405	2.712	3.004	2.878

Table 4. Density ρ (10^3 kg m^{-3}), C_V (10^6 J m^{-3} K^{-1}), E_0 (10^9 J m^{-3}), thermal conductivity k (W m^{-1} K^{-1}), longitudinal velocity (10^3 m s^{-1}), shear velocity (10^3 m s^{-1}), Debye average velocity (10^3 m s^{-1}) and relaxation time (10^{-12} s) vs. temperature T (K) of $ZrSe_2$.

T(K)	ρ	C_V	E_0	k	V_L	V_S	V_D	τ
300	5.483	5.369	1.238	9.80	4.532	2.229	2.472	8.960
400	5.482	5.433	1.780	7.50	4.477	2.200	2.440	6.951
500	5.481	5.460	2.324	6.00	4.423	2.173	2.410	5.769
600	5.480	5.477	2.865	5.00	4.370	2.145	2.379	5.028
700	5.479	5.476	3.407	4.30	4.318	2.118	2.350	4.265
800	5.478	5.485	3.970	3.50	4.263	2.090	2.318	3.560
900	5.477	5.484	4.518	3.00	4.215	2.066	2.291	3.124

Table 5. Average Grüneisen number for longitudinal wave, square of average Grüneisen number for longitudinal wave, average of square of Grüneisen number for longitudinal and shear wave and acoustical coupling constants for longitudinal and shear wave vs. temperature T (K) of ZrS_2.

T(K)	$\langle\gamma_i^j\rangle_L$	$\langle\gamma_i^j\rangle_L^2$	$\langle(\gamma_i^j)^2\rangle_L$	$\langle(\gamma_i^j)^2\rangle_S$	D_L	D_S
300	−0.694	0.482	6.390	0.122	55.472	1.102
400	−0.694	0.482	6.375	0.123	55.491	1.108
500	−0.694	0.482	6.368	0.123	55.520	1.112
600	−0.694	0.482	6.360	0.124	55.511	1.117
700	−0.694	0.482	6.352	0.124	55.483	1.122
800	−0.694	0.482	6.335	0.126	55.360	1.134
900	−0.694	0.482	6.335	0.126	55.386	1.134

Table 6. Average of Grüneisen number for longitudinal wave, square of average Grüneisen number for longitudinal wave, average of square of Grüneisen number for longitudinal and shear wave and acoustical coupling constants for longitudinal and shear wave vs. temperature T(K) of $ZrSe_2$.

T(K)	$\langle\gamma_i^j\rangle_L$	$\langle\gamma_i^j\rangle_L^2$	$\langle(\gamma_i^j)^2\rangle_L$	$\langle(\gamma_i^j)^2\rangle_S$	D_L	D_S
300	−0.689	0.475	5.964	0.195	51.825	1.757
400	−0.689	0.475	5.951	0.198	51.057	1.789
500	−0.689	0.474	5.937	0.202	51.696	1.822
600	−0.688	0.474	5.923	0.206	51.680	1.855
700	−0.688	0.474	5.909	0.209	51.587	1.889
800	−0.688	0.473	5.895	0.213	51.491	1.924
900	−0.688	0.473	5.881	0.217	51.384	1.959

The sound velocities for longitudinal and shear modes in ZrS_2 are 5817 and 2931 m/s while in $ZrSe_2$ they are 4532 and 2229 m/s at 300 K. As the temperature increases, the velocities of the longitudinal and shear waves decrease for both ZrS_2 and $ZrSe_2$. The ultrasonic velocities of ZrS_2 are greater than that of $ZrSe_2$ because the values of elastic constants of the former crystal are greater than that of the latter.

The average of the Grüneisen number for the longitudinal wave, the square of the average Grüneisen number for the longitudinal wave, the average of the square of the Grüneisen number the longitudinal and shear waves, and acoustical coupling constants for the longitudinal wave (D_L) and the shear wave (D_S) have also been evaluated for ZrS_2 and $ZrSe_2$. The evaluated values are presented in tables 5 and 6, respectively.

From tables 5 and 6, it is clear that the value of D_L is greater than D_S for all temperatures indicating that the conversion of ultrasonic energy into thermal energy for the shear ultrasonic wave is less than that of the longitudinal ultrasonic wave.

The variation of angle-dependent ultrasonic velocities for longitudinal wave, quasishear wave, shear wave and Debye average velocity for ZrS_2 is shown in figures 1–4, respectively.

The variation of angle-dependent ultrasonic velocities for longitudinal wave, quasishear wave, shear wave and Debye average velocity for $ZrSe_2$ is shown in figures 5–8, respectively. The variation of the angle-dependent thermal relaxation time for ZrS_2 is shown in figure 9. The variation of the angle-dependent thermal relaxation time for $ZrSe_2$ is shown in figure 10.

The variation of angle-dependent ultrasonic velocities for ZrS_2 and $ZrSe_2$ indicates that the velocity of the longitudinal wave (V_1) has a minimum at 50° with the unique axis, but in the case of the quasishear wave V_2

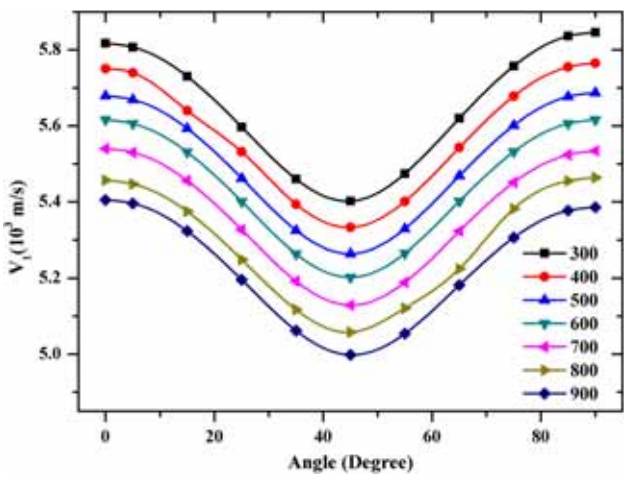

Figure 1. Variation of ultrasonic velocities for longitudinal wave vs. angle at different temperatures for ZrS_2.

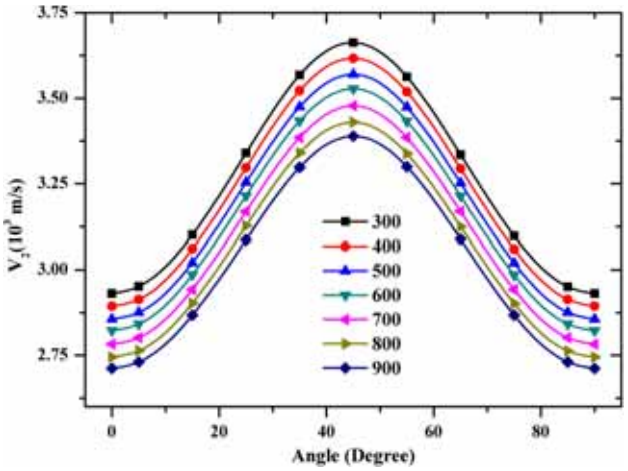

Figure 2. Variation of ultrasonic velocities for quasishear wave vs. angle at different temperatures for ZrS_2.

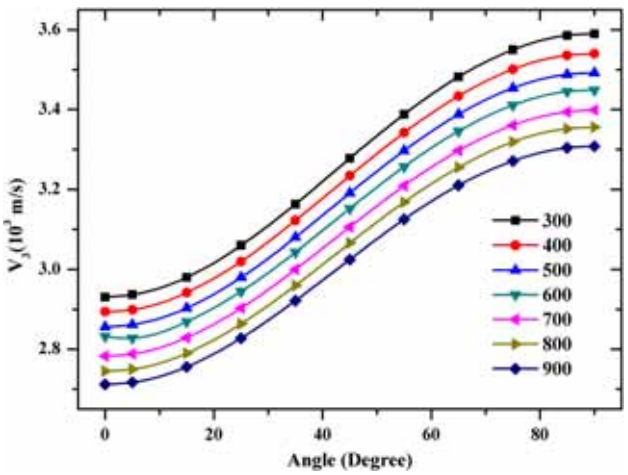

Figure 3. Variation of ultrasonic velocities for shear wave vs. angle at different temperatures for ZrS_2.

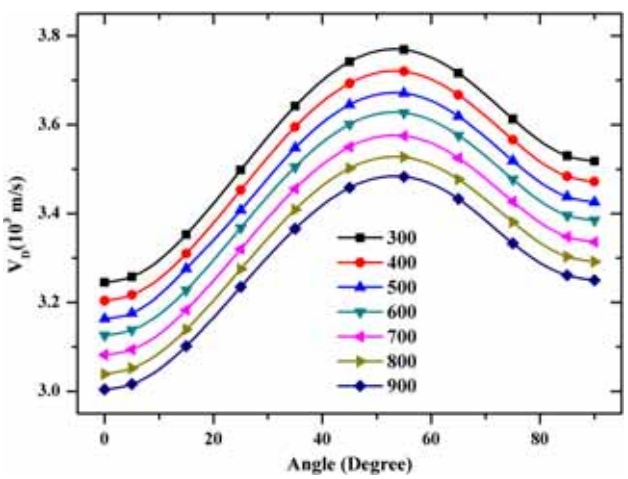

Figure 4. Variation of Debye average velocity vs. angle at different temperatures for ZrS_2.

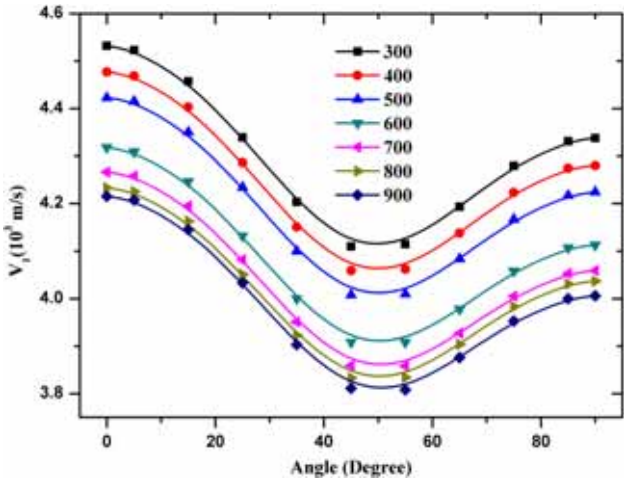

Figure 5. Variation of ultrasonic velocities for longitudinal wave vs. angle at different temperatures for $ZrSe_2$.

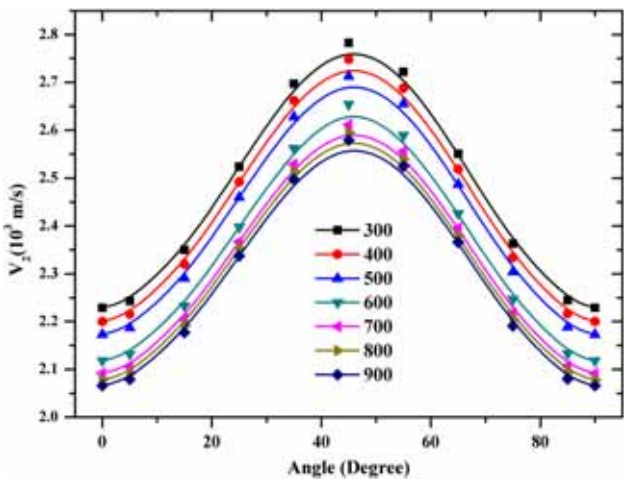

Figure 6. Variation of ultrasonic velocities for quasishear wave vs. angle at different temperatures for $ZrSe_2$.

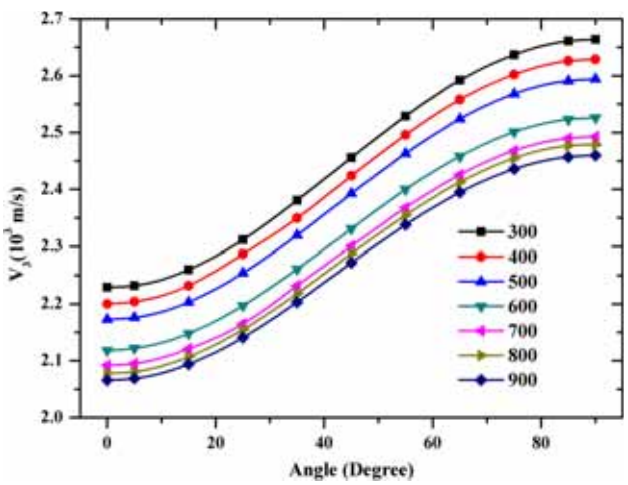

Figure 7. Variation of ultrasonic velocities for shear wave vs. angle at different temperatures for $ZrSe_2$.

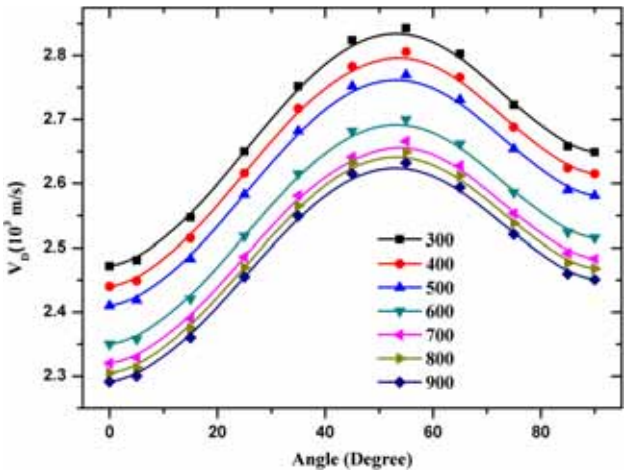

Figure 8. Variation of Debye average velocity vs. angle at different temperatures for $ZrSe_2$.

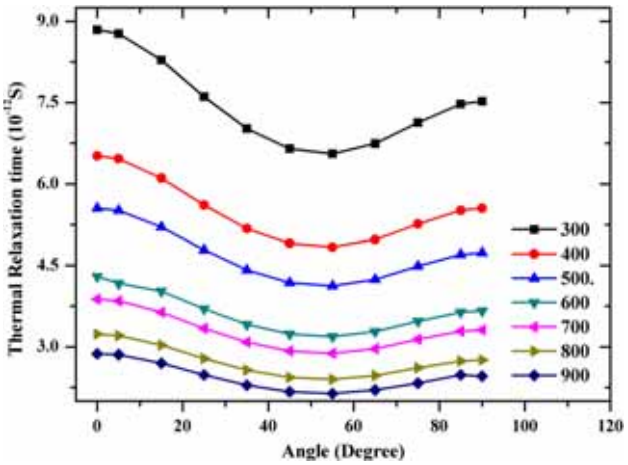

Figure 9. Variation of thermal relaxation time vs. angle at different temperatures for ZrS_2.

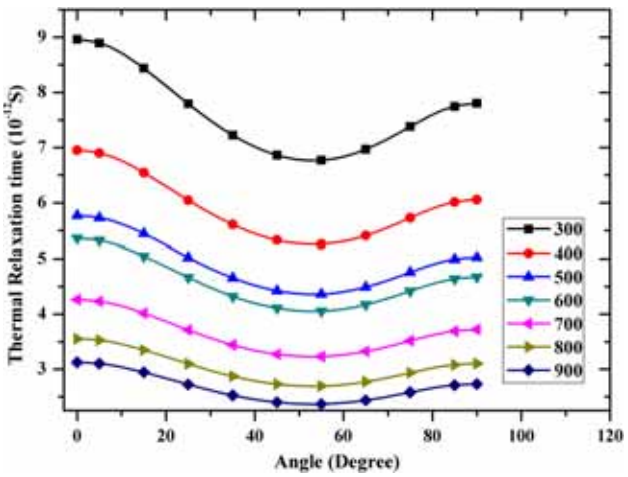

Figure 10. Variation of thermal relaxation time vs. angle at different temperatures for $ZrSe_2$.

Table 7. Ultrasonic attenuation vs. temperature T(K) of ZrS_2.

T (K)	$(\alpha/f^2)_{Th}\times10^{-18}$	$(\alpha/f^2)_{L}\times10^{-15}$	$(\alpha/f^2)_{S}\times10^{-15}$
300	2.037	2.132	0.165
400	2.120	2.404	0.188
500	2.357	2.824	0.222
600	2.285	2.837	0.224
700	2.503	3.192	0.254
800	2.463	3.194	0.259
900	2.573	3.389	0.274

Table 8. Ultrasonic attenuation vs. temperature T (K) of $ZrSe_2$.

T(K)	$(\alpha/f^2)_{Th}\times10^{-18}$	$(\alpha/f^2)_{L}\times10^{-15}$	$(\alpha/f^2)_{S}\times10^{-15}$
300	2.629	2.961	0.422
400	2.849	3.425	0.498
500	3.076	3.692	0.548
600	3.340	4.279	0.649
700	3.421	4.467	0.692
800	3.377	4.489	0.711
900	3.455	4.647	0.752

has a maximum at 50° with the unique axis while the shear wave velocity (V_3) increases with the angle of the unique axis. The variation of thermal relaxation time also shows a minimum at 50° with the unique axis at room temperature, but at higher temperature it is nearly constant because the variation of thermal conductivity at higher temperature is also constant.

The variation of velocities and the relaxation time of ZrS_2 and $ZrSe_2$ are the same as for the other HCP-structured materials like RuCo alloys and third-group nitrides [8,18]. Hence our theoretical approach for calculating angle-dependent velocities and relaxation time with the unique axis for HCP-structured ZrS_2 and $ZrSe_2$ materials is justified and validated.

The ultrasonic attenuation over the frequency square for the longitudinal wave $(\alpha/f^2)_L$ and the shear wave $(\alpha/f^2)_S$ under the condition $\omega\tau \ll 1$ and the attenuation due to thermoelastic loss $(\alpha/f^2)_{Th}$ have also been calculated for ZrS_2 and $ZrSe_2$ in the temperature range 300–900 K and the calculated values are presented in tables 7 and 8, respectively.

The variation of the calculated values of temperature-dependent total ultrasonic attenuation coefficients over the frequency square $(\alpha/f^2)_{total}$ vs. temperature under the condition $\omega\tau \ll 1$ for ZrS_2 and $ZrSe_2$ is shown in figure 11.

While calculating ultrasonic attenuation, it is assumed that the ultrasonic wave is propagating along the unique axis $\theta = 0°$ of the material. The Akhieser-type loss

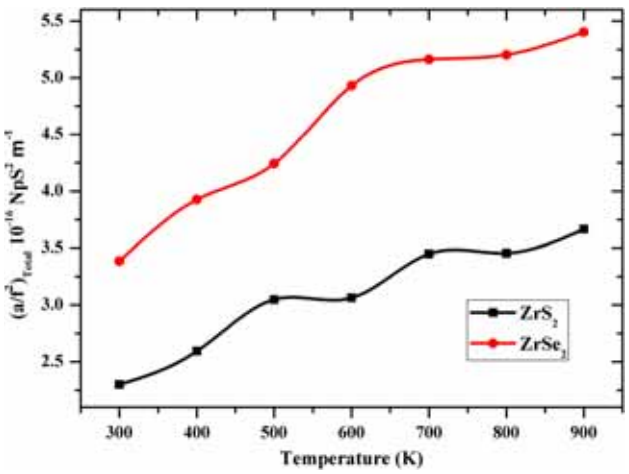

Figure 11. Variation of total ultrasonic attenuation coefficient over frequency square $(\alpha/f^2)_{total}$ vs. temperature for ZrS_2 and $ZrSe_2$.

(attenuation of ultrasonic wave due to phonon–phonon interaction) for ZrS_2 has a lower value in comparison with $ZrSe_2$. The reason behind this is the lower value of the ratio of the thermal relaxation time (τ) to the cube of ultrasonic velocity (V^3) for ZrS_2 in comparison with $ZrSe_2$ as given by eq. (8). The relaxation time mainly depends on thermal conductivity (k) and Debye average velocity (V_D) as given by eq. (11). In the case of thermoelastic loss, it is mainly affected by thermal conductivity (k) and longitudinal ultrasonic velocity (V_L) as given by eq. (13). Total ultrasonic attenuation over frequency square increases with temperature despite the decrease in thermal conductivity because of the dominating effect of energy density which increases with the same. The total ultrasonic attenuation over frequency square for ZrS_2 shows slight minima at 600 K because the product of energy density and thermal conductivity also shows the same behaviour around this temperature while in the case of $ZrSe_2$, there is no such unusual variation of thermal conductivity.

4. Conclusions

On the basis of the above discussion, the following conclusions can be drawn:

- The theory using simple interaction potential model for the evaluation of temperature-dependent nonlinear higher-order elastic constants and ultrasonic attenuation is validated for the TE HCP crystal ZrX_2.
- The order of thermal relaxation time for ZrX_2 is found in picoseconds, which justifies their HCP structure.

- Temperature-dependent thermal conductivity and energy density are core factors in determining the nature of temperature-dependent total ultrasonic attenuation in ZrX_2.
- The conversion of acoustic energy into thermal energy will be large for ZrS_2 in comparison with $ZrSe_2$.

The study may be useful for the processing and online characterisation of similar HCP-structured materials. The results of the present evaluations elucidate correlations between the ultrasonic properties and figure of merit of the studied TE crystalline materials, which may be relevant for solving various energy problems.

Acknowledgement

The author (S P Singh) is thankful to the UGC, New Delhi, India for the financial support.

References

[1] P K Dhawan, M Wan, S K Verma, D K Pandey and R R Yadav, *J. Appl. Phys.* **117**, 074307 (2015)
[2] Q Zhao, Y Guo, K Si, Z Ren, J Bai and X Xu, *Phys. Status Solidi B* **254**, 1700033 (2017)
[3] X Wang, L Huang, X W Jiang, Y Li, Z Wei and J Li, *J. Mater. Chem. C* **4**, 3143 (2016)
[4] Y Ōnuki, S Yamanaka, R Inada, M Kido and S Tanuma, *Synth. Met.* **5**, 245 (1983)
[5] G Yumnam, T Pandey and A K Singh, *J. Chem. Phys.* **143**, 234704 (2015)
[6] G Ding, G Y Gao, Z Huang, W Zhang and K Yao, *Nanotechnol.* **27**, 375703 (2016)
[7] S M Valero, V G López, A Cantarero and M Galbiati, *Appl. Sci.* **6**, 264 (2016)
[8] P K Yadawa, D Singh, D K Pandey, G Mishra and R R Yadav, *Adv. Mater. Phys. Chem.* **1**, 14 (2011)
[9] D Singh, D K Pandey, P K Yadawa and A K Yadav, *Cryogenics* **49**, 12 (2009)
[10] D Singh, P K Yadawa and S K Sahu, *Cryogenics* **50**, 476 (2010)
[11] R R Yadav and D Singh, *Intermetallics* **9**, 189 (2001)
[12] K Brugger, *Phys. Rev. A* **133**, 1611 (1964)
[13] S K Kor and R R Yadav and Kailash, *J. Phys. Soc. Jpn.* **55**, 207 (1986)
[14] S Mori and Y Hiki, *J. Phys. Soc. Jpn.* **45**, 1449 (1978)
[15] P B Ghate, *Phys. Rev. A* **139**, 1666 (1965)
[16] J Philip and M A Breazeale, *J. Appl. Phys.* **54**, 752 (1983)
[17] S K Verma, R R Yadav, A K Yadav and B Joshi, *Mater. Lett.* **64**, 1677 (2010)
[18] D K Pandey, D Singh and R R Yadav, *Appl. Acoust.* **68**, 766 (2007)
[19] P K Yadawa, *Pramana – J. Phys.* **76**, 613 (2011)
[20] C P Yadav and D K Pandey, *Pramana – J. Phys.* **92**: 1 (2019)
[21] D K Pandey and R R Yadav, *Appl. Acoust.* **70**, 412 (2009)
[22] D K Pandey, P K Yadawa and R R Yadav, *Mater. Lett.* **61**, 5194 (2007)
[23] P K Dhawan, S Upadhyaya, S K Verma, M Wan, R R Yadav and B Joshi, *Mater. Lett.* **114**, 15 (2014)
[24] W P Mason, *J. Acoust. Soc. Am.* **40**, 852 (1966)
[25] K Brugger and T C Fritz, *Phys. Rev.* **157**, 524 (1967)
[26] M Nandanpawar and S Rajagopalan, *J. Acoust. Soc. Am.* **71**, 1469 (1982)